Hydration Dynamics at Femtosecond Time Scales and Angstrom Length Scales from Inelastic X-Ray Scattering

Robert H. Coridan,[1,†] Nathan W. Schmidt,[1,†] Ghee Hwee Lai,[1,†] Rahul Godawat,[2] Michael Krisch,[3] Shekhar Garde,[2]
Peter Abbamonte,[1] and Gerard C. L. Wong[1,4,*,†]

[1]*Department of Physics, University of Illinois at Urbana-Champaign, Urbana, Illinois 61801, USA*
[2]*Department of Chemical and Biological Engineering, Rensselaer Polytechnic Institute, Troy, New York 12180, USA*
[3]*European Synchrotron Radiation Facility, Grenoble Cedex, France*
[4]*Department of Materials Science and Engineering, University of Illinois at Urbana-Champaign, Urbana, Illinois 61801, USA*
(Received 13 April 2009; published 3 December 2009)

We use high resolution dynamical structure factor $S(q, \omega)$ data measured with inelastic x-ray scattering to reconstruct the Green's function of water, which describes its density response to a point charge, and provides a fundamental comparative model for solvation behavior at molecular time scales and length scales. Good agreement is found with simulations, scattering and spectroscopic experiments. These results suggest that a moving point charge will modify its hydration structure, evolving from a spherical closed shell to a steady-state cylindrical hydration "sleeve".

A molecular understanding of water and solvation dynamics is central to a broad range of phenomena [1–3]. High spatial resolution techniques, such as x-ray absorption spectroscopy [4], x-ray [5] and neutron scattering [6,7], often supplemented with simulations, have elucidated water structure. In a complementary approach, femtosecond water dynamics have been studied using ultrafast spectroscopy in conjunction with simulations [8–12]. Inelastic x-ray scattering (IXS) is a hybrid scattering and spectroscopy technique that measures electron density fluctuations [13–15]. Recently, it has been demonstrated that the IXS measured dynamical structure factor $S(q, \omega)$ at eV resolution can be "inverted" to obtain the Green's function, which allows the dynamics of a system to be reconstructed [16].

Here, we reconstruct the femtosecond dynamics of water at molecular length scales from the Green's function extracted from a library of milli-electronvolt (meV) resolution $S(q, \omega)$ data. This high resolution data set, measured over a data range coextensive with the present limits of 3rd generation synchrotron x-ray sources, enables this Green's function imaging of dynamics (GFID) approach to track the average oxygen-density correlations in water at 26 fs temporal resolution and at 0.44 Å spatial resolution. The recovery and reintegration of causality into the $S(q, \omega)$ measurement allowed us to order the observed excitations in time, and consequently reconstruct dynamics. This is analogous to a solution of the "phase" problem, which reconstructs a crystal structure from a set of diffraction intensities by recovering the lost phase. The extracted Green's function, also known as the density-density response function $\chi(q, \omega)$, is a direct measure of water response to an ideal point charge, and provides a new data-based perspective to solvation processes. This Green's function can be used to reconstruct spatiotemporal water dynamics around dynamic charge distributions, particularly those governed by Gaussian statistics, valid at length scales smaller than those that nucleate a change in phase in the surrounding solvent [17–19]. GFID results are compared to diffraction experiments, classical molecular dynamics (MD) simulations of diffusional relaxation, and to femtosecond spectroscopic measurements. To illustrate the potential of GFID, we also reconstruct the evolving hydration structure around an accelerating point charge moving near thermal velocity. Rather than the often assumed abstraction of spherically-symmetric hydration shells that rigidly follow a moving charge, these results indicate that charge movement strongly modifies the hydration structure, which evolves from a closed spherical shell to a steady-state hydration "sleeve" with cylindrical symmetry.

IXS data were measured at Beamline ID-28 of the European Radiation Synchrotron Facility (ESRF), with an incident x-ray energy of 21.747 keV ($\Delta E \sim 1.7$ meV, Si(11, 11, 11) reflection). The step size in q of 0.15 Å^{-1} is larger than the q resolution of each measurement (0.03 Å^{-1}). Data from 6.1 Å^{-1} to 7.5 Å^{-1} were collected on the same instrument using the higher intensity Si(9,9,9) reflection with incident energy 17.794 keV ($\Delta E \sim 3.0$ meV). Because of the width of measured features at large q, this resolution difference has a negligible effect, confirmed by comparing identical measurements with different resolutions. The dynamic structure factor of room temperature and pressure liquid water $S(q, \omega)$ was measured for energies to 80 meV over a q range from 0.2 Å^{-1} to 7.2 Å^{-1}, which is an unusually large data set for IXS. Future work can address anomalous water behavior via $S(q, \omega)$ libraries measured at specific (P,T) conditions [5,15,20]. After removing the empty cell contribution, the raw data was normalized to an energy-integrated measurement of the intensity $I(q)$.

The function $S(q, \omega)$ quantifies the correlation of density fluctuations in a given medium [21]. The fluctuation-

dissipation theorem relates $S(q, \omega)$ to the imaginary part of the linear response function $\chi(q, \omega) = \chi'(q, \omega) + \iota\chi''(q, \omega)$, where $\chi''(q, \omega) = -\pi[S(q, \omega) - S(q, -\omega)]$. Since the measured $S(q, \omega)$ can be weak, we use the detailed balance relationship, $S(q, -\omega) = e^{-\beta\omega}S(q, \omega)$ [21] to relate χ'' to S. After correcting for finite resolution [22], each measured spectrum was divided by the Bose factor $n(\omega) = (1 - e^{-\hbar\omega/kT})^{-1}$ to yield $\chi''(q, \omega)$ [Fig. 1(a)]. $\chi'(q, \omega)$ is calculated from $\chi''(q, \omega)$ using Kramers-Kronig (KK) relations as previously described [16,21]. KK relations and Fourier transforms require that the argument functions be defined on an infinite continuous domain. We extended the data onto a continuous interval using linear interpolation to avoid artifacts from discrete data sets. The IXS data at the endpoints of our measurements in q and in ω are essentially featureless and at background count levels. We extrapolated this data to infinity using an optimized two-mode damped harmonic oscillator (DHO) model function [13]. The best-fit DHO model parameters were consistent with those reported in other IXS experiments on water. The known acoustic phonon mode with a sound velocity of 3190 m/s is observed at low q values as expected [13,14]. The extrapolated data in ω corresponds to times before the first time step at 50 fs in the reconstructions, and does not significantly influence results in the time regime of interest.

The full $\chi(q, \omega)$ is Fourier transformed into the real space response function $\chi(r, t)$ [Fig. 1(b)]. Several snapshots of $\chi(r, t)$ are shown, which indicate the induced water density at a distance r and time t after exposure to a delta function charge perturbation at the origin. The lack of an isotopic shift for D_2O relative to H_2O [13] shows that $S(q, \omega)$ measured here is dominated by motion of the center of mass of the water molecule [15]. After the delta

function impulse at $t = 0$, the water density relaxes in the form of transient "hydration ripples". The amplitude of the density fluctuations is at maximum after $t \sim 100$ fs, and decays back to equilibrium. Residual density fluctuations are essentially indistinguishable from zero after $t \sim 1$ ps.

The experimental energy and momentum resolution places fundamental limits on the spatiotemporal resolution, as well as the spatiotemporal range over which phenomena may be observed with GFID. The sampling density in the energy of the measurement is much smaller than the energy resolution of the instrument ($\Delta E = 1.7$ meV), and limits the maximum time window to $2\pi/\Delta E = 2.8$ ps. Likewise, in reciprocal space, the q resolution of the instrument ($\Delta q = 0.03$ Å^{-1}) is finer than the spacing between measurement points (~ 0.15 Å^{-1}), which indicates that the maximum object size is $2\pi/0.15$ Å$^{-1} = 41$ Å. We calculate the baseline spatiotemporal resolution via the Nyquist condition based on the highest ω and q measured [23], yielding $\Delta t = \pi/80$ meV = 26 fs and $\Delta r = \pi/7.2$ Å$^{-1} = 0.44$ Å.

We use GFID to reconstruct the equilibrium ($t \sim \infty$) hydration structure around an idealized negative point charge, which is given by the spherical Fourier transform of $\chi(q, \omega = 0)$ [Fig. 1(c)]. Since we measure the longitudinal response, the radial displacement of water molecules can be detected. The hydration density profile indicates formation of defined hydration shells. Since there are no true point charges in reality, we cannot compare the position of the first hydration shell to that in a physically realizable ion. The distance between the first and second shells ($r = 2.6$ Å), however, agrees with that measured from bulk water using x-ray diffraction (2.65 Å) [5].

The nanoscopic diffusive relaxation dynamics of water can be reconstructed using GFID. We use linear response theory to calculate the induced charge density $\delta n_{ind}(\mathbf{q}, \omega)$ due to an external time-dependent charge density $\delta n_{ext}(\mathbf{q}, \omega)$ by:

$$\delta n_{ind}(\mathbf{q}, \omega) = \frac{4\pi^2 e^2}{q^2}\chi(q, \omega)\delta n_{ext}(\mathbf{q}, \omega). \quad (2)$$

This induced charge density is essentially a measure of the time-dependent average induced oxygen density in water. We track relaxation of the hydration structure for $t > 0$, following the removal of a point charge at $t = 0$ from a fully hydrated structure [Fig. 2(a)]. The equilibration of density at the origin and in the first hydration shell can be fit to exponentials with time constants of 113 fs and 125 fs, respectively. The density returns to the equilibrium bulk value after ~ 500 fs. We compare this to density response averaged over 1000 MD simulation trajectories from ion-water systems in which an ion is removed at $t = 0$ from an equilibrated system [Fig. 2(b)]. The water density profile initially shows typical water packing around an ion, with well-developed solvation peaks. After ion removal, the profile relaxes to bulk density via orientational relaxation
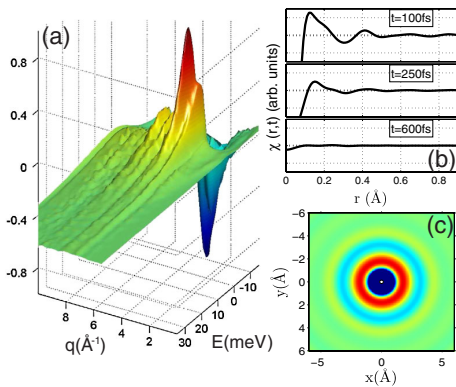

FIG. 1 (color online). (a) The complete measurement of $\chi''(q, \omega)$ for water at ambient conditions. (b) The response function $\chi(r, t)$ at 100 fs, 250 fs, and 600 fs. At ~ 600 fs after the impulse, the hydration ripples have dissipated. (c) A 2D representation of the hydration structure around a point negative charge. Red (medium gray), [blue (dark gray)] represents an accumulation [depletion] of oxygen density with respect to bulk. The distance between the first and second hydration shells is $r = 2.6$ Å, which compares well with that measured for bulk water.

and translational diffusion, leading to a decay of the profile and filling of the ion cavity. The temporal relaxation of the first hydration peak height is approximately exponential with time constants for different cations and anions in the 60–90 fs range [Fig. 2(c)], displaying slightly faster relaxation than in GFID results. This may be reasonable given that the SPC/E water model typically overestimates the water diffusion constant. Because of the asymmetry of charge distribution in water, and correspondingly of the hydration structures, a difference in the relaxation dynamics is observed for cations and anions. These results highlight limitations of GFID in its simplest implementation, which does not take into account excluded volume effects of finite-sized ions. Also, GFID intrinsically does not

account for the cation-anion hydration asymmetry. Although the present comparison is limited by the use of classical MD simulations, the similarity of structural features and relaxation time scales indicate that the basic physics is captured in MD and in GFID.

X-ray probes like GFID are particularly sensitive to water oxygen dynamics. In our $\chi(q, t)$ data, underdamped density oscillations can be seen for length scales larger than the 3 Å ($q < 2$ Å^{-1}), roughly the distance between two O atoms in water. In the q range shown, these oscillations have a period that varies between 250 fs and 180 fs, decreasing with increasing q [Fig. 2(d)]. Inversions of the best-fit functions from the extrapolation procedure are also shown (solid lines) to verify that the oscillations result from the dispersive modes of the dynamic structure factor. For the length scales close to 3 Å, a density fluctuation period of $\sim$200 fs is close to the measured 170 fs period of ($q = 0$) O-O oscillation between water molecules from femtosecond IR absorption spectroscopy [12]. Interestingly, for larger q values corresponding to intramolecular distances, this oscillation mode vanishes, consistent with an intermolecular O-O feature.

Femtosecond hydration dynamics can be seen in the real space response of water to a periodic perturbation. We reconstruct the behavior of water in the presence of a THz-frequency amplitude monopole at the origin using $\delta n_{ext}(\mathbf{r}, t) = \delta(\mathbf{r}) \sin(2\pi t/T)$. The steady-state dynamical hydration structure can be calculated as the spherical Fourier transform of $\chi(q, \omega = 2\pi/T)\chi(q, \omega = -2\pi/T)$. For a driven harmonic oscillator, the system oscillates with the driving period, but lags the driving monopole by a phase shift $\phi(\omega) = \tan^{-1}(\chi''(\omega)/\chi'(\omega))$ [Fig. 2(e), inset]. For comparison, we try to fit the measured phase shift to that of a harmonic oscillator in a viscous fluid [24], $\tan\phi(\omega) = \omega\gamma/(\omega_0^2 - \omega^2)$, where ω_0 is the resonant frequency and γ the viscous damping of the fluid. Clearly, the harmonic oscillator model does not fit the behavior of water over the full range of periods. For high driving frequencies ($T \ll 100$ fs), the water response at the origin lags behind the oscillator by a smaller than expected phase shift. As the driving period increases, (100 fs $< T <$ 200 fs), this phase shift increases drastically. Limited agreement with driven harmonic oscillator models is observed for $T \gg 200$ fs [Fig. 2(e)]. The fit resonant frequency ω_0 of 17.2 meV implies a temporal period of 240 fs, consistent with the reconstructed range of values for O-O oscillation above for this q range.

The phase shifts reconstructed from GFID deviate from the harmonic oscillator for rapid oscillations ($T < 120$ fs), indicating a different regime of response. This can be seen in the "flattening out" of the slope in the phase shift ϕ for small T [Fig. 2(e)]. Simulation and spectroscopic experiments have observed that water has two modes of molecular response: a fast mode from inertial motions that occur on the scale of tens of femtoseconds, and a slow mode due to diffusional repositioning, occurring on the scale of
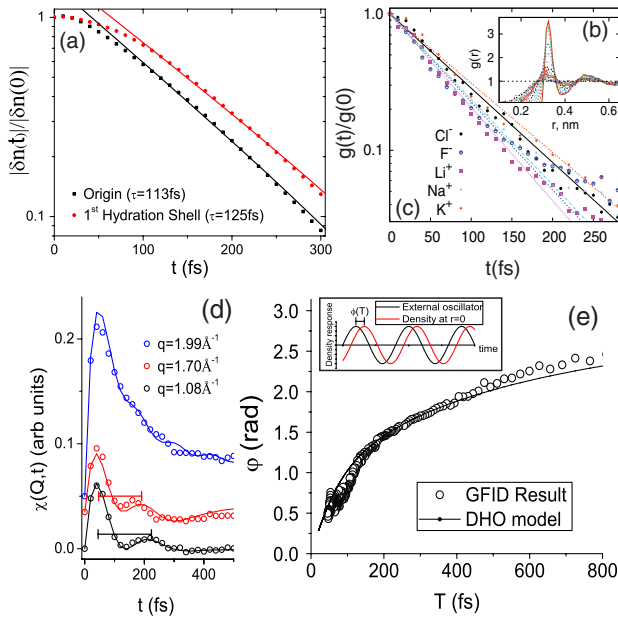

FIG. 2 (color online). Diffusional relaxation of water structure in response to the removal of an ion is compared to MD simulations. (a) After ion removal the GFID reconstructed density returns to the bulk value at the origin (black) and in the first hydration shell (red) exponentially with time constants $\tau = 113$ fs and 125 fs (solid lines, fit for $t > 50$ fs), respectively. (b) MD radial distribution function $g(r, t)$ of water oxygens: 15 different profiles are shown for $t = 0, 20, 40, \ldots, 280$ fs. (c) Normalized first peak height $g_{max}(t)$, shown as $\Delta g(t)/\Delta g(0) = (g_{max}(t) - 1)/(g_{max}(0) - 1)$, is obtained for five ion types. Fit exponential time constants vary from 64 fs (for Li$^+$) to 86 fs (for K$^+$). (d) $\chi(q, t)$ from IXS data (open symbols) show underdamped density oscillations for intermolecular distances ($q < 2$ Å^{-1}) but not for intramolecular distances ($q > 2$ Å^{-1}). For each q value, the corresponding curve from the best-fit DHO model is shown. The temporal period of this mode varies between 250 fs (black bar) and 180 fs (red bar) at (1.08 Å$^{-1} < q < 1.7$ Å^{-1}), consistent with an O-O oscillation (e) For a sinusoidal driving frequency of an amplitude monopole, the steady-state induced density lags by phase $\phi(T)$. For $T \gg$ 200 fs, $\phi(T)$ can be approximated by the phase lag of a damped, driven harmonic oscillator (solid line). For $T \ll 200$ fs, the behavior deviates strongly from the harmonic oscillator.
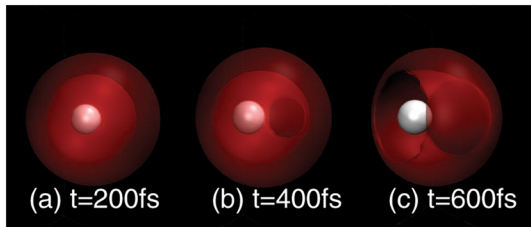
FIG. 3 (color online). (a–c) The evolution of hydration structure around a point charge (white sphere) as it accelerates harmonically to $v_0 = 500$ m/s in 500 fs. 3D renderings were generated using the software package VMD [25].

hundreds of femtoseconds [8]. Although it does not prove their existence, the behavior of phase shifts from GFID is consistent with this picture of two modes.

We use GFID to examine inertial effects by reconstructing movies (Fig. 3) of the evolving hydration structure around an idealized point charge accelerating harmonically in a THz field [$v(t) = v_0 \sin(\omega t)$, $v_0 = 500$ m/s, $\omega = 2\pi/2$ ps]. The hydration structure is indicated by regions of oxygen-density enhancement [red (medium gray)]. Three snapshots from the first 600 fs show the evolution of the hydration shell as the speed increases from 0 to v_0. The original spherically-symmetric hydration is progressively replaced by a weakly ordered hydration "sleeve" of cylindrical symmetry. At times less than 100 fs after initiation of linear movement, there is weak but observable relaxation of the spherically-symmetric hydration structure, as the leading edge of the shell thins. As v increases to v_0, the electron distribution breaks through the first hydration shell, which exhibits significant longitudinal distortion along the axis of movement, which requires asymmetric radial reorganization of oxygen density. At ~500 fs, the hydration structures equilibrate into the steady-state cylindrical hydration sleeve, followed by a trail of depressed oxygen density with a velocity-dependent length. These results suggest that a stationary molecule and a moving molecule may participate in chemical reactions in water differently.

In summary, we have used GFID to extract the Green's function of water from IXS data, which is a direct measure of hydration behavior around a point charge. Good agreement is found with extant experiments and simulations. It is known that effects such as density saturation around highly charged sources can affect linear response. In future work, we will compare GFID results to quantum MD simulations.

*Corresponding author: gclwong@illinois.edu
†Present address: Department of Bioengineering, CNSI, UCLA, Los Angeles, CA 90095.

[1] A. Luzar and D. Chandler, Nature (London) **379**, 55 (1996).
[2] Y.-K. Cheng and P. J. Rossky, Nature (London) **392**, 696 (1998).
[3] D. A. Zichi and P. J. Rossky, J. Chem. Phys. **84**, 2814 (1986).
[4] P. Wernet et al., Science **304**, 995 (2004).
[5] T. Head-Gordon and G. Hura, Chem. Rev. **102**, 2651 (2002).
[6] A. H. Narten and H. A. Levy, J. Chem. Phys. **55**, 2263 (1971).
[7] A. K. Soper and M. G. Phillips, Chem. Phys. **107**, 47 (1986).
[8] R. Jimenez, G. R. Fleming, P. V. Kumar, and M. Maroncelli, Nature (London) **369**, 471 (1994).
[9] S. Woutersen, U. Emmerichs, and H. J. Bakker, Science **278**, 658 (1997).
[10] S. Woutersen and H. J. Bakker, Nature (London) **402**, 507 (1999).
[11] J. B. Asbury et al., J. Chem. Phys. **121**, 12431 (2004).
[12] C. J. Fecko et al., Science **301**, 1698 (2003).
[13] F. Sette et al., Phys. Rev. Lett. **75**, 850 (1995).
[14] F. Sette et al., Phys. Rev. Lett. **77**, 83 (1996).
[15] G. Ruocco and F. Sette, J. Phys. Condens. Matter **11**, R259 (1999).
[16] P. Abbamonte, K. D. Finkelstein, M. D. Collins, and S. M. Gruner, Phys. Rev. Lett. **92**, 237401 (2004).
[17] L. R. Pratt and D. Chandler, J. Chem. Phys. **67**, 3683 (1977).
[18] G. Hummer et al., Proc. Natl. Acad. Sci. U.S.A. **93**, 8951 (1996).
[19] G. E. Crooks and D. Chandler, Phys. Rev. E **56**, 4217 (1997).
[20] P. H.-L. Sit et al., Phys. Rev. B **76**, 245413 (2007).
[21] D. Pines and P. Nozieres, *The Theory of Quantum Liquids* (W. A. Benjamin, Inc., Reading, MA, 1966), Vol. 1.
[22] The sharp quasielastic peak ($\omega \approx 0$, width <1 meV) is resolution broadened in measured spectra, which can lead to density artifacts. To eliminate this effect, the Lorentzian term of the DHO fit function centered at $\omega = 0$ corresponding to the quasielastic line was subtracted from each measured spectrum. Since this term is symmetric, it does not contribute to χ''. Extrapolation in q was done after the time transform, and the line shape of $\chi(q, t)$ was fit to a series of Gaussian peaks to capture the measured profile while enforcing the condition that $\chi(q) \to 0$ smoothly for large q.
[23] P. Abbamonte et al., Proc. Natl. Acad. Sci. U.S.A. **105**, 12159 (2008).
[24] P. M. Chaikin and T. C. Lubensky, *Principles of Condensed Matter Physics* (Cambridge University Press, Cambridge, UK, 1995).
[25] W. Humphrey, A. Dalke, and K. Schulten, J. Mol. Graphics **14**, 33 (1996).